UC San Diego

UC San Diego Electronic Theses and Dissertations

Title

Using Human Embryonic Stem Cells to Model Maturity-Onset Diabetes of the Young Type 1 (MODY1)

Permalink

https://escholarship.org/uc/item/9np5c3nv

Author

Lin, Hu-An

Publication Date

2019

Peer reviewed|Thesis/dissertation

eScholarship.org Powered by the California Digital Library
University of California

UNIVERSITY OF CALIFORNIA SAN DIEGO

Using Human Embryonic Stem Cells to Model Maturity-Onset Diabetes of the Young Type 1 (MODY1)

A thesis submitted in partial satisfaction of the requirements
for the degree of Master of Science

in

Biology

by

Hu-An Lin

Committee in Charge:

Professor Maike Sander, Chair
Professor Randolph Hampton, Co-Chair
Professor David Traver

2019

Copyright

Hu-An Lin, 2019

All rights reserved.

The thesis of Hu-An Lin is approved and it is acceptable in quality and form for publication on microfilm and electronically:

Co-Chair

Chair

University of California San Diego

2019

DEDICATION

I dedicate this thesis to my family, for their unconditional love, trust, support, and encouragement.

TABLE OF CONTENTS

SIGNATURE PAGE..... iii

TABLE OF CONTENTS v

LIST OF FIGURES vi

LIST OF TABLES vii

ACKNOWLEDGEMENTS viii

ABSTRACT OF THE THESIS ix

INTRODUCTION 1

RESULTS 8

MATERIALS AND METHODS 28

REFERENCES.....38

LIST OF FIGURES

Figure 1. Generation of hESC-derived beta cells carrying *HNF4α*^{R141X} mutation..... 16

Figure 2. **HNF4α expression decreases in *HNF4α*^{R141X} mutants**. 17

Figure 3. Representative images of hESC-derived beta cell morphology at different stages of differentiation..... 18

Figure 4. *HNF4α*^{R141X} mutation does not affect pancreatic induction. 19

Figure 5. *HNF4α*^{R141X} mutation results in a transient decrease in insulin+/NKX6.1+ cell population at immature beta cell stage 1 (IMB1). 20

Figure 6. *HNF4α*^{R141X} mutants exhibit hyperinsulinism and diazoxide-responsiveness at the immature beta cell stage 2 (IMB2). 22

Figure 7. *HNF4α*$^{R141X/+}$ mutant secrete more insulin in response to high glucose level at the functionally mature beta cell stage (FMB). 23

Figure 8. *HNF4α*^{R141X} mutants may be more prone to cell death. 24

LIST OF TABLES

Table 1. List of Plasmids and Primers 34

Table 2. List of Antibodies for Immunofluorescence Staining 35

Table 3. List of Flow Cytometry Antibodies 36

Table 4. Krebs-Ringer-Bicarbonate Solution for Perfusion Assay 37

ACKNOWLEDGEMENTS

First, I would like to thank Dr. Maike Sander for giving me the opportunity to join her lab. My time at the Sander lab not only has widened my understanding for the research field, but also sparked my interest in studying medical research. Dr. Sander has provided me with guidance and encouragement whenever it was needed.

I would also like to thank Dr. David Traver and Dr. Randolph Hampton for taking the time to serve as members of my thesis committee.

Next, I would like to thank all the members of the Sander lab. I would especially like to thank Kim-Vy Nguyen-Ngoc for her mentorship and support. This project would not have been possible without her guidance.

Lastly, I would like to thank all my family and friends for their unconditional support and encouragement.

ABSTRACT OF THE THESIS

Using Human Embryonic Stem Cells to Model Maturity-Onset Diabetes of the Young Type 1 (MODY1)

by

Hu-An Lin

Master of Science in Biology

University of California San Diego, 2019

Professor Maike Sander, Chair
Professor Randolph Hampton, Co-Chair

Maturity-onset diabetes of the young type 1 (MODY1) is a form of monogenic diabetes caused by single base pair mutation in the hepatocyte nuclear factor-4-alpha (*HNF4α*) gene that results in neonatal hyperinsulinemic hypoglycemia, macrosomia, and early onset diabetes. Although many *HNF4α* mutations have been identified in patients and their families, the molecular mechanism of MODY1 progression remains unknown. This study aims to understand the mechanism underlying *HNF4α* R141X mutations in pancreatic beta cells using human embryonic stem cell (hESC)-derived beta cells and genome editing CRISPR/Cas9 technology. By

differentiating hESCs into insulin-producing beta cells using a stepwise protocol, we found that *in vitro* generated beta cells carrying the R141X mutation show phenotypes similar to clinical presentation of MODY1. At the immature stage, which is likely equivalent to the neonatal stage *in vivo*, mutant beta cells hypersecrete insulin at low glucose, which can be reduced by treatment of the potassium channel activator diaxozide. At the stage when wild-type (WT) beta cells become functionally mature and secrete insulin in response to glucose levels, HNF4α mutants hypersecrete insulin in both low and high glucose conditions. At both stages, mutant beta cells consistently secrete higher insulin in response to KCl-induced depolarization than WT. Furthermore, RNA sequencing of immature beta cells revealed upregulation of genes involved in cell cytotoxicity in R141X mutants. This is validated by an increase in cleaved Caspase-3 in mutants, suggesting that *HNF4*α-mutated cells might be prone to cell death. Overall, our results show that hESC-generated R141X mutant beta cells behave similarly to beta cells from MODY1 patients and this mutation may induce apoptosis in beta cells.

INTRODUCTION

Diabetes Mellitus

Diabetes mellitus is a metabolic disease characterized by hyperglycemia, insulin resistance, and abnormal insulin secretion [1]. In 2017, the Centers of Disease Control and Prevention (CDC) named it as the 7th leading cause of death in the United States, affecting approximately 30.3 million people in the United States and 387 million worldwide [2,3]. Patients with diabetes mellitus often suffer short-term complications such as polyuria, weight loss, blurred vision, ketoacidosis, and long-term complications such as retinopathy, nephropathy, peripheral neuropathy, and cardiovascular symptoms [1].

Diabetes mellitus is classified into several categories based on clinical presentation and physiological cause of symptoms. Diabetes mellitus can be classified as into two broad categories: type I diabetes, type II diabetes; however, there are other less prevalent forms of diabetes that cannot be classified as either type 1 or type 2 diabetes.

The first classification, type I diabetes (T1D), is commonly caused by autoimmune responses that result in the destruction of beta cells, pancreatic endocrine cells located in the islets of Langerhans in the pancreas that produce insulin to maintain glucose homeostasis [4]. Due to beta cell loss, the body experiences insulin deficiency, leading to disruption in glucose homeostasis and resulting in hyperglycemia. Patients with T1D are required to supply the body with exogenous insulin regularly and maintain glucose monitoring [5]. While T1D patients have insulin injection as an option for symptom treatment, there is currently no cure for the disease. Current research for T1D focuses on expanding treatment options and developing ways to achieve early diagnosis to prevent beta cell loss [4].

Type II diabetes (T2D), on the other hand, accounts for 90-95% of all diabetes cases and is characterized by insulin resistance, relative insulin deficiency, and dysregulation of carbohydrate, lipid, and protein metabolism [1,2,6]. T2D is mainly due to progressive beta cell dysfunction that is accompanied by insulin resistance in skeletal muscle, liver, and adipose tissue [5]. Furthermore, DeFronzo and colleagues established the "ominous octet", which identifies major dysfunctions in insulin secretion, glucagon secretion, neurotransmitter secretion, peripheral glucose uptake, renal glucose excretion, hepatic glucose output, and incretin secretion as core causes of hyperglycemia and insulin resistance [6]. Insulin resistance in these tissues requires beta cells to hyper-secrete insulin to compensate for this condition, leading to prolonged cell stress that gradually leads to beta cell dysfunction or apoptosis. T2D patients are advised to maintain a healthy low-fat diet and moderate exercise, which have been proven to improve glycemia [8]. The complexity of T2D often requires patients to use multiple medications to manage individual conditions. Most antidiabetic medications target specific parts of the insulin release pathway. These antidiabetic medications include, but are not limited to, metformin, sulfonylureas, thiazolidinediones (TZD), dipeptidyl peptidase 4 (DPP4) inhibitors, sodium-glucose cotransporter 2 (SGLT2) inhibitors, α-glucosidase inhibitors (AGIs), glucagon-like peptide 1 (GLP1) receptor agonists, and insulin injection [9].

Other types of diabetes that do not match the diagnosis of T1D and T2D include various less prevalent subtypes of diabetes. These types of diabetes may be caused by genetic defects in beta cells, genetic defects in insulin action, exocrine pancreas damage, endocrinopathies, external drugs or chemicals, infection, and pregnancy [1]. Some examples include Rabson-Mendenhall syndrome and maturity on-set diabetes of the young (MODY). The former caused by genetic defects in the insulin receptor and latter caused by genetic defects of specific genes expressed in

beta cells. This heterogeneity of diabetes presents challenges for scientists to study diabetes as a single disease but also poses issues for clinicians to diagnosis the disease correctly for proper treatment.

Maturity-Onset Diabetes of the Young (MODY)

Much of our early understandings of diabetes mechanisms came from studies of monogenic diabetes, or diabetes caused by mutations in a single gene [14]. One such form is called MODY, a monogenic diabetes that accounts for 1-4% of all diabetes [10]. MODY is an autosomal-dominant disease that is characterized by hyperglycemia before the age of 25 and insulin secretion defects [11]. According to Online Mendelian Inheritance in Man (OMIM), there are currently 14 variants of MODY identified, each caused by a specific gene [12]. Each type of MODY can have a different clinical presentation, which includes neonatal hyperinsulinism, pancreas agenesis, pancreas hypoplasia, and diabetes in infancy or early adulthood [12]. Of the 14 variants, four genes account for majority of the MODY cases: hepatocyte nuclear factor-4-alpha (*HNF4α*)/MODY1, glucokinase (*GCK*)/MODY2, hepatocyte nuclear factor-1-alpha (*HNF1α*)/MODY3, and hepatocyte nuclear factor-1-beta (*HNF1β*)/MODY5 [13]. Studies on MODY have aided our understanding of the molecular mechanisms of diabetes. For example, it has been shown that homozygous mutation in GCK impairs glucose-dependent ATP production and inhibition of K_{ATP} channel closure, suggesting GCK as a key glucose sensor [15]. Early studies in pancreatic and duodenal homeobox 1 (*PDX1*)/MODY4 have found that single base pair deletion in *PDX1* results in pancreatic agenesis, a congenital malformation of the pancreas that results in a failure of the dorsal pancreas to develop, suggesting *PDX1* is a critical regulator of pancreatic development [16].

Clearly, while MODY has relatively low prevalence comparing to T2D, it provides extremely valuable models to study diabetes.

Compared to other major MODY genes, much less is known about *HNF4α* mutations and its mechanism. This is likely due to its relatively low prevalence, as only 103 mutations and 174 families with the disease have been identified to date [17]. MODY1 is characterized by heterozygous point mutation in *HNF4α* with clinical features of neonatal hyperinsulinemic hypoglycemia (HH), macrosomia, and early onset diabetes [18]. Patients with neonatal HH are treated with diazoxide, a potassium channel activator that inhibits insulin release from beta cells, ranging from 3 months to 8 years of life [19]. In their mid-20s, most *HNF4α* carriers develop MODY and are commonly treated with sulfonylurea, a drug that closes ATP-sensitive potassium channels in beta cells to initiate insulin release. However, studies have shown that it is an effective treatment for only 75-80% of the patients and patients develop unresponsiveness after 3-25 years of treatment [20,21]. In addition, there is no report of patients' health in between these two treatments, presenting a gap of knowledge.

HNF4α is a transcription factor in the nuclear receptor (NR) superfamily with conserved DNA-binding domains and ligand-binding domains [22,23]. It encodes two isoforms from two different promoters, P1 and P2. P1 variant is expressed in the kidney, intestine, colon, and liver. It is the most abundant DNA-binding protein in liver, binding to more than 40% of actively transcribed genes, suggesting its vital role in hepatocyte differentiation and function [24]. The second variant, P2 is mainly expressed in the pancreas, intestine, and colon. Transfection assays with various deletions and mutations of the P2 promoter have shown that this isoform is a master regulator of pancreas gene expression, interacting with many other MODY transcription factors such as HNF1β, HNF1α, and PDX1 [25,26]. Specifically, studies have shown that HNF4α

regulates beta cell replication in response to increased metabolic demand via the Ras/ERK pathway and endoplasmic reticulum (ER) calcium ion homeostasis via X-box binding protein-1 (Xbp1) [27,28]. Many familial studies have confirmed that mutations in *HNF4α* lead to MODY in humans [29-31]. However, while beta cell-specific *HNF4α*-null mice exhibit impaired glucose-stimulated insulin secretion, these mice do not develop diabetes like their human counterpart [32]. The discrepancy between the mouse model and clinical presentation of MODY1 patients makes the mouse model a less reliable resource to study how *HNF4α* mutation causes MODY1, highlighting the importance to develop a human *in vitro* model to study MODY1.

Beta Cell Differentiation from Human Embryonic Stem Cells (hESCs)

There has been great interest in the field to generate beta cells from human embryonic stem cells (hESCs) and human induced-pluripotent stem cells (iPSCs) as a potential therapy for diabetes. While patients have the option to receive islet transplantation, it is limited by the availability of donors. Islet transplantation also presents many health risks, as patients are required to take immunosuppressant drugs for as long as the transplanted islets are functional. As a result, much effort has been placed to generate functional beta cells from hESCs and iPSCs as an alternative and renewable source of islet transplantation. In addition to transplantation, *in vitro* derived beta cells can be utilized for drug screening and disease modeling.

The major approach in the last decade is to model the path pluripotent cells take during embryogenesis to become mature beta cells. *In vitro*, hESCs are exposed to growth factors that resemble developmental cues *in vivo*, allowing the cells to go through developmental stages from definitive endoderm (DE), primitive gut tube (GT), posterior foregut (PF), pancreatic endoderm (PE), endocrine progenitor (EP), immature beta cell (IMB) 1 and 2, to finally functionally mature

beta cell (FMB) [33-37]. Despite rigorous effort to perfect the protocol, researchers face many challenges in generating mature glucose-responsive beta cells *in vitro*. Studies have shown that multiple factors other than growth factor cues affect beta cell development and function. For instance, isolated beta cells have compromised GSIS as oppose to intact islets, suggesting cell-cell communication with other islet endocrine cells plays a role in insulin secretion regulation [38]. In addition, other non-endocrine cells such as endothelial cells, perivascular cells, neuronal cells, and mesenchymal cells have also been suggested to play a role in beta cell function. For example, endothelial cells have been suggested to be a critical modulator of beta cell growth, survival, and function, as it synthesizes islet basement membrane to maintain islet vasculature [39]. Despite many limitations of the hESC-derived beta cell model, it serves as an extremely valuable tool to study diabetes such as MODY1, where the phenotype is different between humans and rodents. Recent studies have placed emphasis on generating mono-hormonal insulin positive beta cells with glucose-stimulated insulin secretion (GSIS) and have successfully generating FMB *in vitro*, providing a promising future for diabetes cellular therapies [40,41]

Generating a Model to Study MODY1 Using hESC-Derived Beta Cells

It is well established that monogenic heterozygous mutations in *HNF4α* causes MODY1, with the clinical presentation of neonatal HH, macrosomia, and early onset diabetes [18]. However, the underlying cause of how *HNF4α* mutation causes this phenotype remains unclear. With beta cell-specific *HNF4α*-null mice not presenting clinical features observed in humans, the hESC model becomes an extremely valuable tool to study MODY1 [31,32]. Studies have identified 103 mutations in *HNF4α* that result in MODY1, including heterozygous R141X (also termed R154X) mutation, a nonsense point mutation at Arg 141 that results in a truncated protein [17,30]. The

mutation is found in the E domain, which is involved in ligand-binding and dimerization. Studies done in human embryonic kidney 293 cells (HEK 293T) have shown that while the mutation does not affect its DNA binding ability and nuclear localization, the mutant loses 30-100% of its transactivation activity, including impairment in coactivator p300 recruitment [42-44]. To investigate how a single base pair substitution in *HNF4α* is able to cause MODY1, this study aims to construct a hESC-based model for MODY1 with R141X mutation to provide a tool to investigate the underlying cause of *HNF4α* mutation-mediated diabetes and shed light on potential targets of HNF4α

.

RESULTS

Transfection with dual donors is more efficient in generating R141X heterozygous clones

In order to study the effect of *HNF4α* mutation on beta cells, we attempted to generate a human-embryonic stem cell (hESC) line carrying the *HNF4α* R141X mutation using the H1 cell line (**Figure 1A**). We designed, validated, and inserted a guide RNA (gRNA) that has a binding site near the R141X locus into the plasmid pX458, which already contains Cas9 construct for CRISPR/Cas9 editing and green fluorescent protein (GFP) gene for selection (**Table 1**). To introduce the mutation, we first performed homology directed repair (HDR)-based CRISPR/Cas9 editing by co-transfecting pX458 with one single-stranded DNA (ssDNA) donor carrying two single base changes (mR141X): one for the R141X mutation and one for the protospacer adjacent motif (PAM) sequence mutation. PAM is a short DNA sequence that allows Cas9 nuclease to cut the DNA. By mutating PAM, the allele is protected from further excision by Cas9 nuclease. However, this approach had low efficiency of obtaining truly heterozygous clones, with approximately 0.5% success rate. While we were able to see R141X mutation successfully introduced in one allele, we often found in-dels, or unexpected random insertions or deletions, in the second allele.

To improve this process, we designed and introduced an additional ssDNA donor that contains only the PAM mutation (R141X) (**Table 1**). We co-transfected pX458 with mR141X ssDNA donor and R141X ssDNA donor in the hopes that this will protect the wild-type allele from addition excision and random in-dels. With this dual donor system, the efficiency for generating the *HNF4α* R141X heterozygous clone increased to 2% (data not shown (**Figure 1B**)).

HNF4α expression decreases in *HNF4α*^{R141X} mutants

Many studies have shown that HNF4α plays a crucial role for endodermal organogenesis. During development, HNF4α is first expressed at the gut tube stage. It is involved in crosstalk with other transcription factors that are important in islet differentiation, such as HNF1α and FOXA [45,46]. It remains expressed in adult beta cells to mediate insulin secretion, gluconeogenesis, and lipid metabolism [47-49]. In order to assess the expression level of HNF4α protein in wild-type and mutant beta cells at different developmental stages, we differentiated hESCs into beta cells using a stepwise protocol (**Figure 1C**). We first wanted to verify HNF4α expression in these genotypes by immunofluorescent staining (IF) and Western blot. Using an antibody that recognizes the HNF4α C-terminus domain, we detected HNF4α signal at the PE stage in the nucleus in wild-type and *HNF4α*$^{R141X/+}$ cells, but not in *HNF4α*$^{R141X/R141X}$ cells (**Figure 2A-B**). In *HNF4α*$^{R141X/+}$ cells, HNF4α signal intensity was lower than in wild-type cells (**Figure 2A-B**). It is important to note that there is a clonal difference between *HNF4α*$^{R141X/+}$ clone 1 and *HNF4α*$^{R141X/+}$ clone 2. With both methods, *HNF4α*$^{R141X/+}$ clone 1 had lower HNF4α expression than *HNF4α*$^{R141X/+}$ clone 2.

We then assessed the expression level of HNF4α protein in our cells at different developmental stages. We observed a similar pattern of HNF4α expression levels in *HNF4α*$^{R141X/+}$ relative to the wild-type at the EP and IMB1 stages (**Figure 2A, C-D)**. In wild-type cells, HNF4α protein levels decreased as beta cells was further differentiated from the PE stage to the IMB1 stage (**Figure 2B-D**). However, the level of reduction was more severe in *HNF4α*$^{R141X/+}$ mutants compared to wild-type cells (**Figure 2E**). Moreover, the levels of HNF4α of *HNF4α*$^{R141X/+}$ clone 1 resembled that of HNF4α$^{R141X/R141X}$ mutants at the IMB1 stage (**Figure 2D**). While HNF4α expression is reduced in *HNF4α*^{R141X} clones, the cell aggregate morphology between the wild-type and the clones are similar throughout GT, PF, PE, and IMB1 stages (**Figure 3**). These data

indicated that while *HNF4α* mutation exacerbates HNF4α protein reduction during beta cell differentiation, the mutations do not affect morphogenesis during pancreatic induction.

The INS+/NKX6.1+ cell population is transiently reduced in *HNF4α*^{R141X} cells

We next examined whether *HNF4α* R141X mutation affects pancreatic induction by using immunofluorescence (IF) staining and fluorescence-activated cell sorting (FACS) to check expression of PE-specific markers. We found that there was no difference in pancreatic and duodenal homeobox 1 (PDX1) and NKX6 homeobox 1 (NKX6.1) expression between *HNF4α* mutants and WT control (**Figure 4**). Quantification data by IF staining combined with image analysis and FACS show similar results, despite the fact that image analysis showed a slightly higher percentage of NKX6.1+, which was due to different sensitivities of the two antibodies used in the two methods (**Figure 4B-C).** These quantification data further suggest that *HNF4α* R141X mutations do not affect pancreas induction.

Next, we assessed whether *HNF4α* R141X mutation affect beta cell specification by staining the differentiated cells at EP, IMB1, and IMB2 stages with NKX6.1 and insulin (INS). At the EP stage, we observed the cells began to express INS and the percentage of NKX6.1+ cells increased by 30% compared to PE cells (**Figure 4B-C, 5A, D, E**). The quantification data shows that the percentage of INS+ cells were relatively similar between the wild-type control and the *HNF4α*^{R141X} clones, which was around 50-70% across all genotypes and quantification methods (**Figure 5D-E**). In addition, there was a slight reduction of NKX6.1+ cells and INS+/NKX6.1+ cells at the EP, IMB1, and IMB2 stages in the mutants compared to wild-type cells at each corresponding stage, although statistical significance was not observed consistently between the two methods of quantification.

At the IMB1 stage, we expected to see an increase in INS+ cells and INS+/NKX6.1+ cell populations compared to the EP stage. Across all genotypes, we observed a visible increase in INS+ cells and INS+/NKX6.1+ cells (**Figure 5A-B**). The quantification data showing the difference in NKX6.1+ and INS+/NKX6.1+ cell populations between wild-type and the mutant clones became more obvious when comparing IMB-staged cells to cells at the EP stage (**Figure 5D-G**). *HNF4α*-mutated clones had significantly less NKX6.1+ and INS+/NKX6.1+ cells than wild-type controls, with the homozygous clones exhibiting a lower percentage of these cells than their heterozygous counterparts (**Figure 5D-G**). This raised the question whether this reduction in INS+/NKX6.1+ population may lead to developmental defects in beta cells at the later stages. We questioned whether this difference is maintained as the cells are matured further to the IMB2 stage [37, 51-53]. At the IMB2 stage, the difference between $HNF4\alpha^{R141X/+}$ clones and wild-type controls in terms of NKX6.1+ and NKX6.1+/INS+ populations decreased slightly (**Figure 5C**). Similarly, the significance in the difference between INS+/NKX6.1+ populations in wild type and mutant cells was not consistently observed with both quantification methods (**Figure 5H-I**). Altogether, this data suggests that while $HNF4\alpha^{R141X/+}$ clones have a lower percentage of INS+/NKX6.1+ cells at the IMB1 stage, these cells at the later stage are then recovered, suggesting that this difference is only transient and may not affect beta cell differentiation.

$HNF4\alpha^{R141X}$ mutant cells hypersecrete insulin and are responsive to diazoxide treatment

To determine whether the hESC-derived mutant beta cells exhibit the hyperinsulinism phenotype and responsiveness to diazoxide treatment observed in newborn patients, we performed a perfusion assay on IMB2 cell aggregates. It is well established that at low glucose levels, the K_{ATP} channel remains opened and beta cells are repolarized; therefore, insulin secretion is limited

at a minimal level [54]. However, *HNF4α*^{R141X} beta cells had a higher basal level of insulin secretion than wild-type cells (**Figure 6A**). The phenotype was more severe in *HNF4α*$^{R141X/R141X}$ mutants than in the *HNF4α*$^{R141X/+}$ cells. Since diazoxide has been used to treat patients with hyperinsulinism, we next tested if diazoxide treatment could reduce insulin basal levels in *HNF4α*^{R141X} mutant cells [19]. We found that while diazoxide treatment had no effect on wild-type cells, insulin secretion dropped sharply 10 minutes after diazoxide treatment in *HNF4α*^{R141X} clones (**Figure 6A**). This would indicate that the K_{ATP} channels in mutant cells are leaky and cells are partially depolarized.

We next asked whether the leakage of K_{ATP} channels might exacerbate KCl-induced insulin secretion. When perfused with 30 mM KCl to induce cellular depolarization, WT beta cells released approximately 0.5% of the cell's total insulin pool. The total insulin released was elevated in all *HNF4α*^{R141X} mutants to as high as 6.6 fold higher compared to the wild-type (**Figure 6B**). These results suggest that *HNF4α*^{R141X} mutants recapitulate the insulin hypersecretion and diazoxide-responsiveness in MODY1 patients.

Functionally mature *HNF4α*^{R141X} mutant cells hyper-secrete insulin

Although hESC-derived *HNF4α*^{R141X} beta cells at the IMB2 stage have shown hyperinsulinemia, a phenotype normally observed in MODY1 patients, lack of glucose responsiveness in these IMB2 cells indicates their immaturity. This is due to the fact that the differentiation protocol used to generate IMB2 cells does not produce mature beta cells. Therefore, we next tested whether *HNF4α*^{R141X} mutation affects mature beta cells by adapting a recently published protocol that showed that by reducing cell aggregate size at later differentiation stages and culturing the cells in a serum-free and factor-rich environment, the cells are able to increase

glucose-responsiveness without reducing beta cell marker expression [40]. Since homozygous R141X mutation is not found in patients, we only advanced the study with wild-type and *HNF4α*$^{R141X/+}$ differentiated cells. In addition, to carefully and stringently evaluate the phenotype in *HNF4α*$^{R141X/+}$, we chose to carry only the *HNF4α*$^{R141X/+}$ clone 2 since sequencing data of these 2 clones showed that similar transcriptome changes observed in clone 2 was also observed in clone1, but not vice versa (data not shown). To mature the differentiated beta cells, we dissociated and re-aggregated IMB1 cells and cultured the newly-formed aggregates in factor-free media for additional 11-18 days. Wild-type cells at day 11-18 post-reaggregation exhibited similar INS+, NKX6.1+, and INS+/NKX6.1+ percentages as IMB2 staged day 24 aggregates, demonstrating that beta cell markers are maintained with the new adapted protocol (**Figure 5C, H, 7A-C**). In addition, INS+, NKX6.1+, and INS+/NKX6.1+ percentages were similar between wild-type and *HNF4α*^{R141X} mutants, supporting our earlier conclusion that the INS+/NKX6.1+ cell population difference at the IMB1 stage was only a transient effect (**Figure 7C**).

It is well established that adult beta cells secrete insulin in response to elevated glucose levels with two distinct phases – the first phase with a rapid insulin secretion response, and the second phase with a gradual increase in insulin secretion [55]. We first wanted to test whether wild-type beta cells matured with the new protocol could acquire glucose-responsiveness. In the perfusion assay, we observed that wild-type beta cells only secreted 0.005% of total insulin pool and rapidly increased insulin secretion by 5-6 fold within 4-10 minutes after glucose stimulation, resembling the first phase of glucose-stimulated insulin secretion (GSIS) (**Figure 7D**). Furthermore, 20 minutes after glucose stimulation, a minor increase of insulin secretion was observed, resembling the second phase of GSIS. With *HNF4α*$^{R141X/+}$ clone 2, we observed a consistent increase in insulin basal secretion while maintaining first and second phases of glucose

responses. Although *HNF4α*$^{R141X/+}$ beta cells responded to glucose similarly to wild-type, these cells continued to hyper-secrete insulin during glucose stimulation, suggesting that the mutation causes hypersecretion of insulin (**Figure 7D**). In addition, insulin secretion failed to return to basal level prior to glucose stimulation. Similar to beta cells at the IMB2 stage, KCl-induced insulin secretion was elevated in *HNF4α*$^{R141X/+}$ cells compared to the wild-type cells (**Figure 7E**). Taken altogether, these data suggest that *HNF4α*$^{R141X/+}$ mutant cells hypersecrete insulin, which resembles the phenotypic symptoms of newborn patients.

HNF4α$^{R141X/+}$ could cause MODY1 by increasing cell stress and apoptosis

We next sought to understand why the *HNF4α*$^{R141X/+}$ mutation leads to MODY1. A recent study has suggested that lack of HNF4α function in MODY1 patients result in Ca^{2+} signaling and insulin release disruption in beta cells by altering endoplasmic reticulum (ER) Ca^{2+} homeostasis [28]. Many studies have linked increased ER stress, a condition in which the cell is producing proteins at a rate that exceeds its capacity and has unfolded or misfolded protein accumulation, with many diseases such as T2D, cystic fibrosis, and Alzheimer's disease [56-57]. ER stress is even more relevant due to the high engagement of beta cells in insulin production. Several studies have shown that ER stress could induce apoptosis in beta cells [58-59]. Therefore, we hypothesized that insulin hypersecretion could subject *HNF4α*$^{R141X/+}$ cells to increased ER stress, which in turn leads to apoptosis and eventual beta cell loss. To test this hypothesis, we stained IMB2 cell aggregates with cleaved-caspase 3 (c-CAS3), a marker for the apoptosis pathway, to determine whether *HNF4α*$^{R141X/+}$ beta cells are more prone to apoptosis than the wild-type cells. We observed a 2-3-fold increase of c-CAS3+ and INS+/c-CAS3+ cells in *HNF4α*$^{R141X/+}$ beta cells compared to

their wild-type counterparts (**Figure 8A-B**). These results suggest that *HNF4α*$^{R141X/+}$ mutation may result in MODY1 due to increased cell stress and beta cell death.

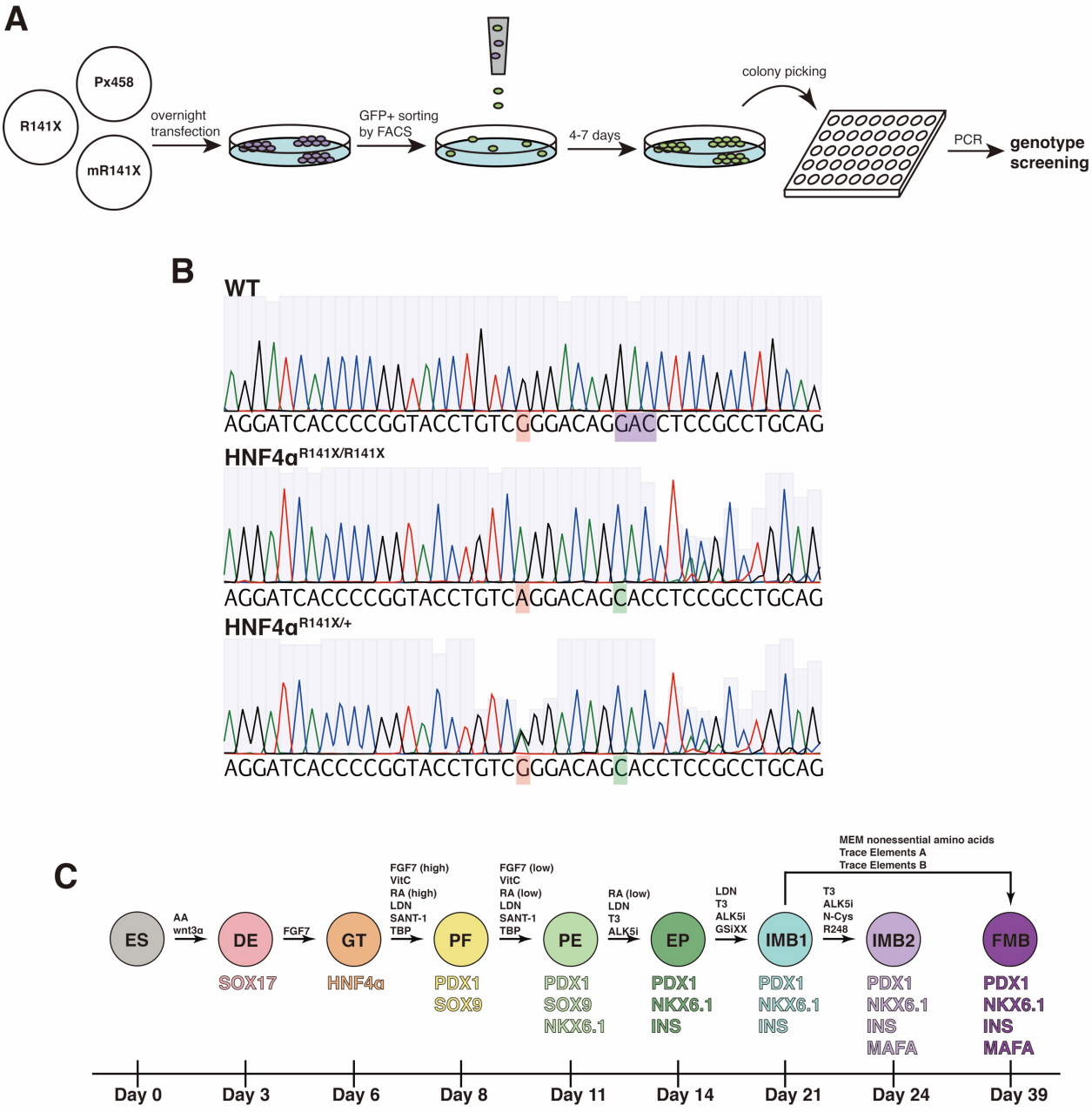


Figure 1. Generation of hESC-derived beta cells carrying *HNF4α*^{R141X} mutation.

(A) Schematic used to generate *HNF4α*^{R141X} mutation in hESCs using CRISPR/Cas9 technology. (B) Chromatogram showing wild-type (WT), homozygous R141X mutant (*HNF4α*$^{R141X/R141X}$), and heterozygous R141X (HNF4α$^{R141X/+}$) genotype. The R141X point mutation is highlighted in red, PAM sequence in purple, PAM point mutation in green. (C) Stepwise protocol to differentiate hESCs into beta cells *in vitro*. The differentiation stages include embryonic stem cells (ES), definitive endoderm (DE), primitive gut tube (GT), posterior foregut (PF), pancreatic endoderm (PE), endocrine progenitor (EP), immature beta cells (IMB), and functionally-mature beta cells (FMB).

…

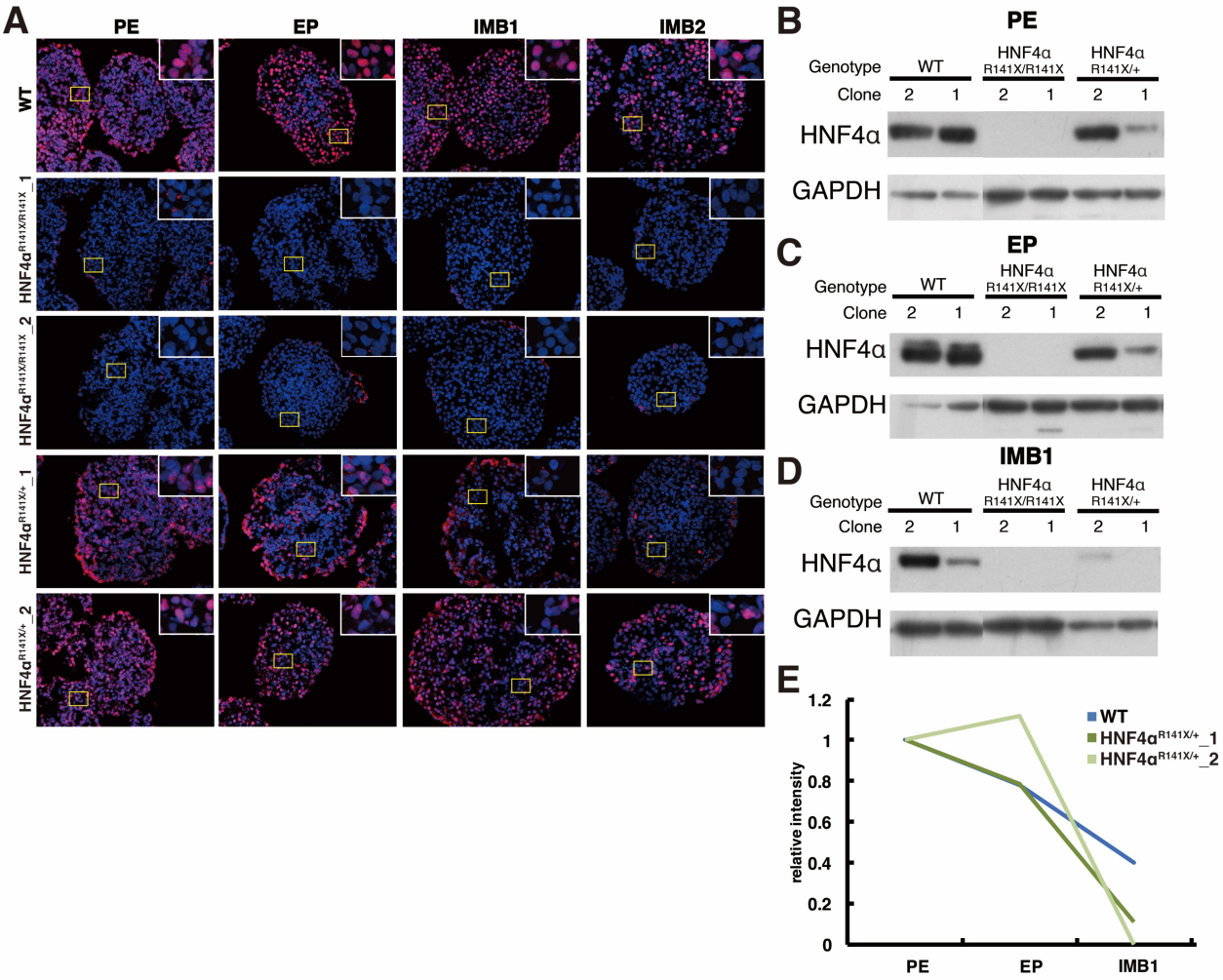


Figure 2. HNF4α expression decreases in *HNF4α*^{R141X} mutants.

(A) Immunofluorescence (IF) staining of HNF4α at different stages of differentiation, including pancreatic endoderm (PE), endocrine progenitor (EP), immature beta cell stage 1 (IMB1), and immature beta cell stage 2 (IMB2). Red stains for HNF4α, blue stains for DAPI. Upper right-hand corner is a 3x magnification of the yellow window. (B-D) Western blot analysis of HNF4α protein at (B) PE, (C) EP, and (D) IMB1 stages. GAPDH is the loading control. (E) Quantification of western blot.

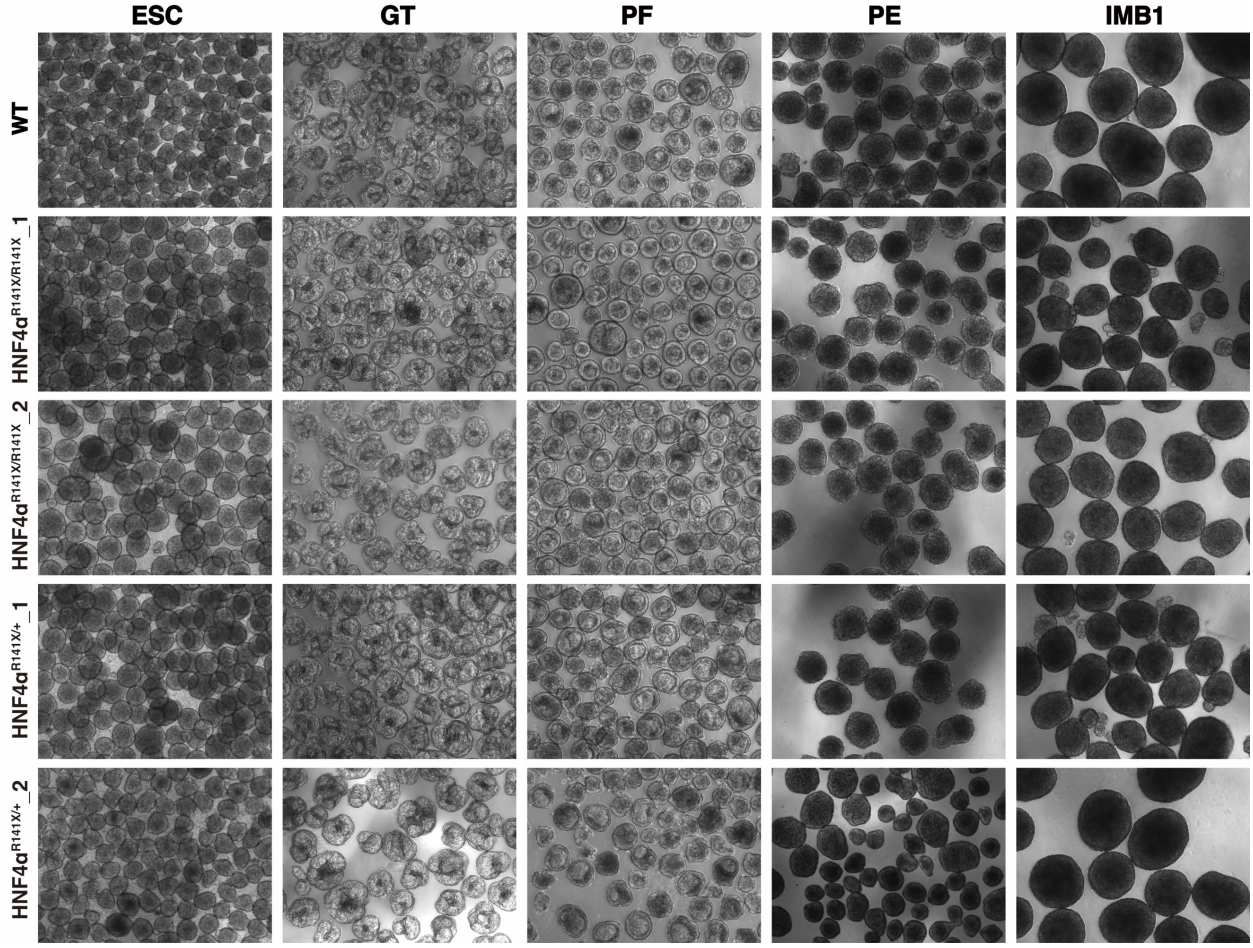


Figure 3. Representative images of hESC-derived beta cell morphology at different stage of differentiation.

Phase contrast images of wild-type (WT) and *HNF4α*^{R141X} mutant aggregates at embryonic stem cells (ES), primitive gut tube (GT), posterior foregut (PF), pancreatic endoderm (PE), endocrine progenitor (EP), immature beta cells (IMB) stages

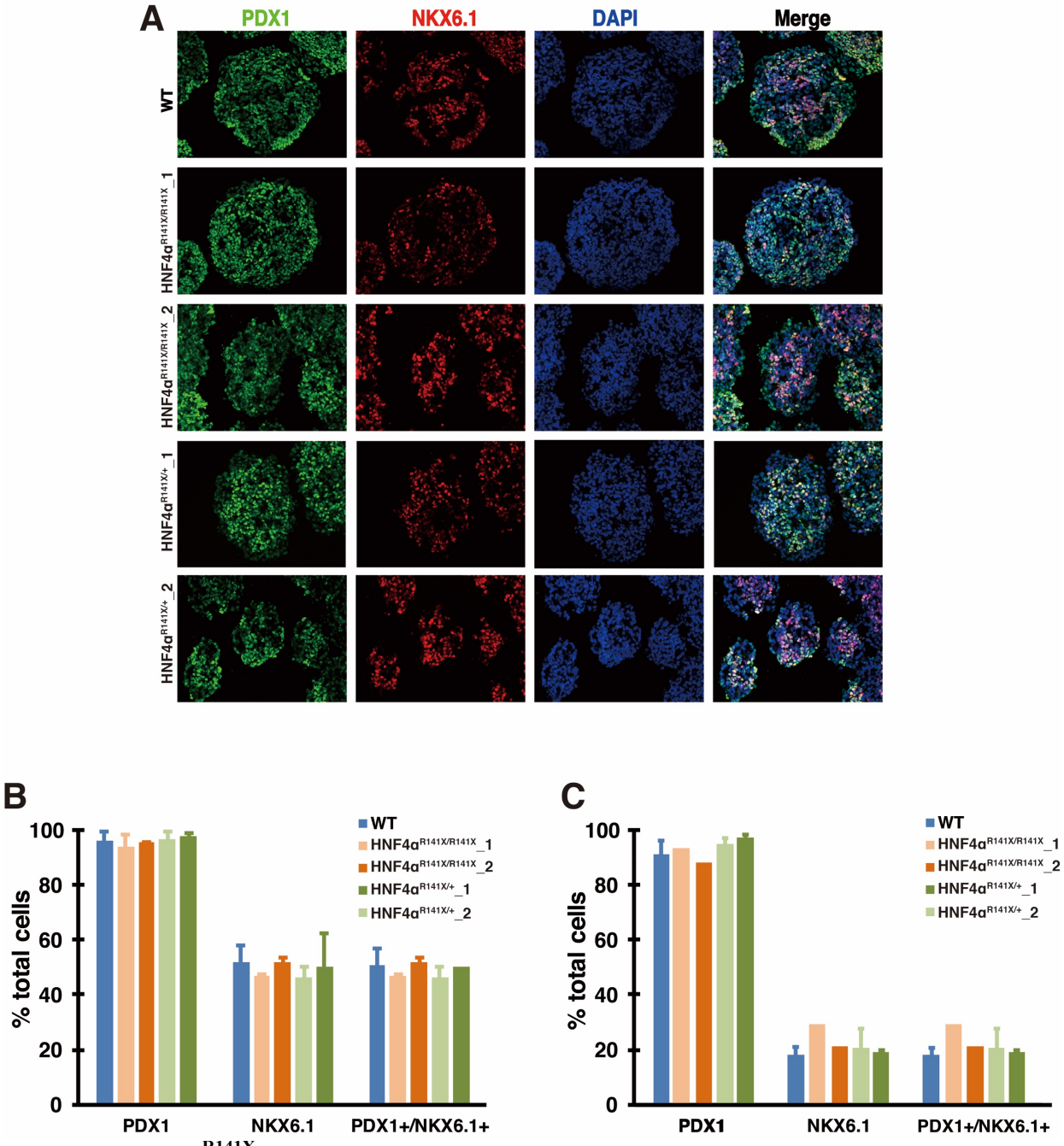
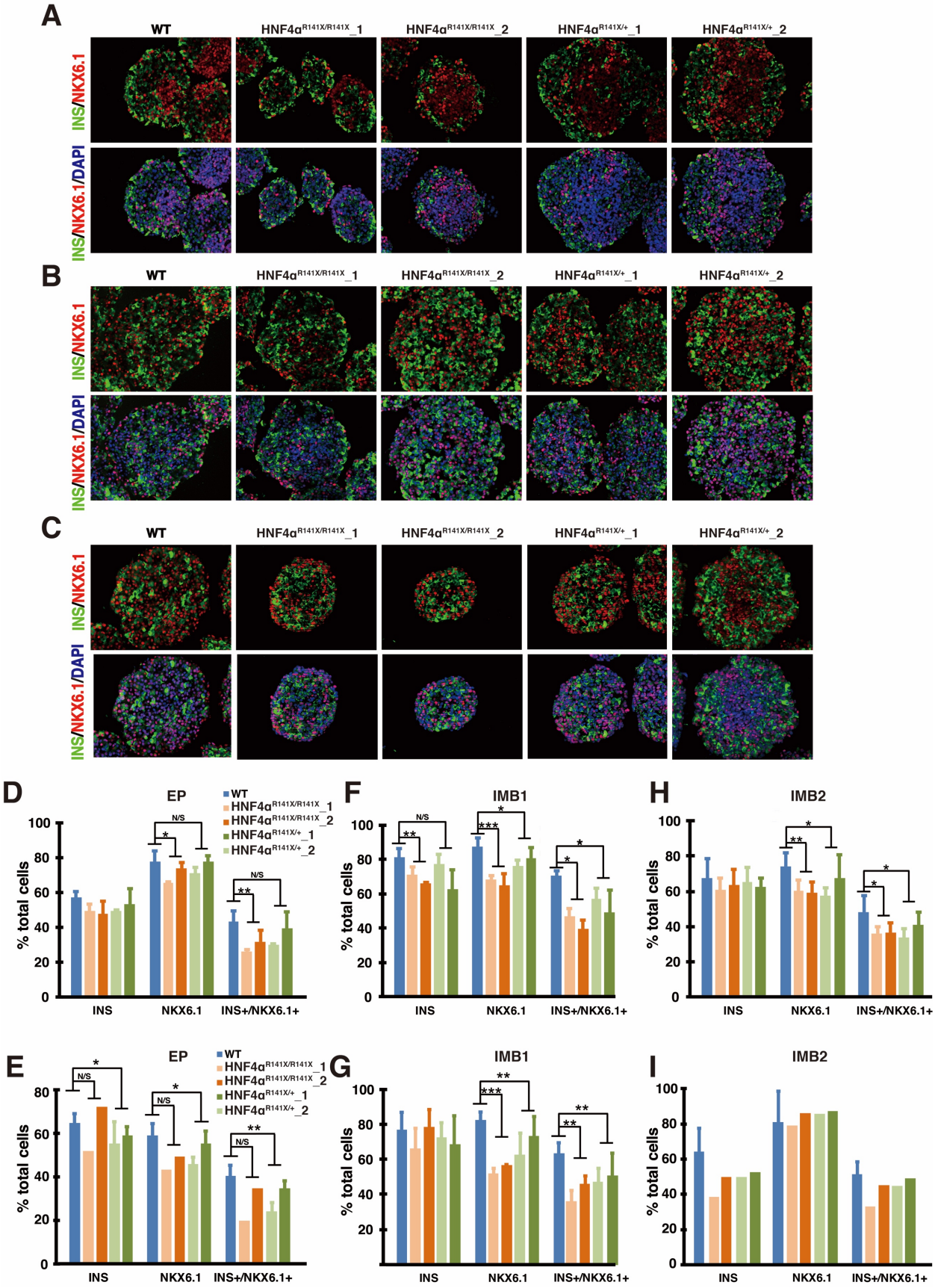


Figure 4. *HNF4α*^{R141X} mutation does not affect pancreatic induction.

(A) IF staining of hESC-derived beta cells at PE stage. Green stains for PDX1, red stains for NKX6.1, blue stains for DAPI. (B) IF staining quantification and (C) FACS quantification of PDX1+, NKX6.1+, and PDX1+/NKX6.1+ cells at PE stage.

Figure 5. *HNF4α*^{R141X} mutation results in a transient decrease in insulin+/NKX6.1+ cell population at immature beta cell stage 1 (IMB1).

(A-C) IF staining of hESC-derived beta cells at (A) EP, (B) IMB1, (C) IMB2 stages. Green stains for insulin (INS), red stains for NKX6.1, blue stains for DAPI. (D,F,H) IF staining quantification of (D) PE, (F) IMB1, and (H) IMB2 cells. (E,G,I) FACS quantification of (E) EP, (G) IMB1, and (I) IMB2 stages. *P<0.05, **P<0.01. ***P<0.001


A
B
C
WT
HNF4α R141X/R141X _1
HNF4α R141X/R141X _2
HNF4α R141X/+ _1
HNF4α R141X/+ _2
INS/NKX6.1
INS/NKX6.1/DAPI
D
EP
F
IMB1
H
IMB2
E
G
I
% total cells
INS
NKX6.1
INS+/NKX6.1+
N/S

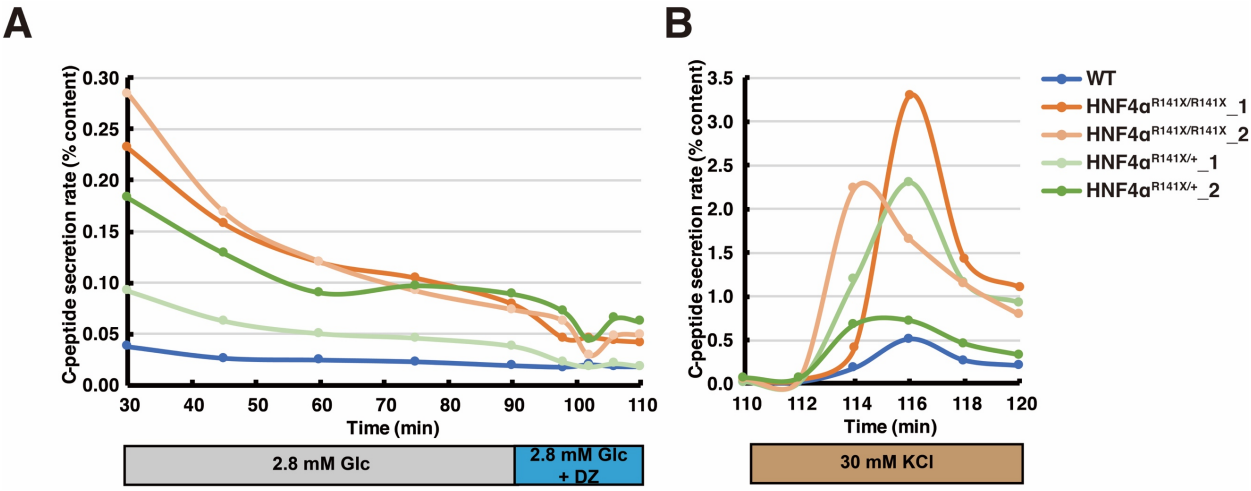


Figure 6. *HNF4α*^{R141X} mutants exhibit hyperinsulinism and diazoxide-responsiveness at the immature beta cell stage 2 (IMB2).

(A-B) Perfusion results of IMB2 cell aggregates with (A) low glucose level and diazoxide treatment (DZ), and (B) KCl treatment.

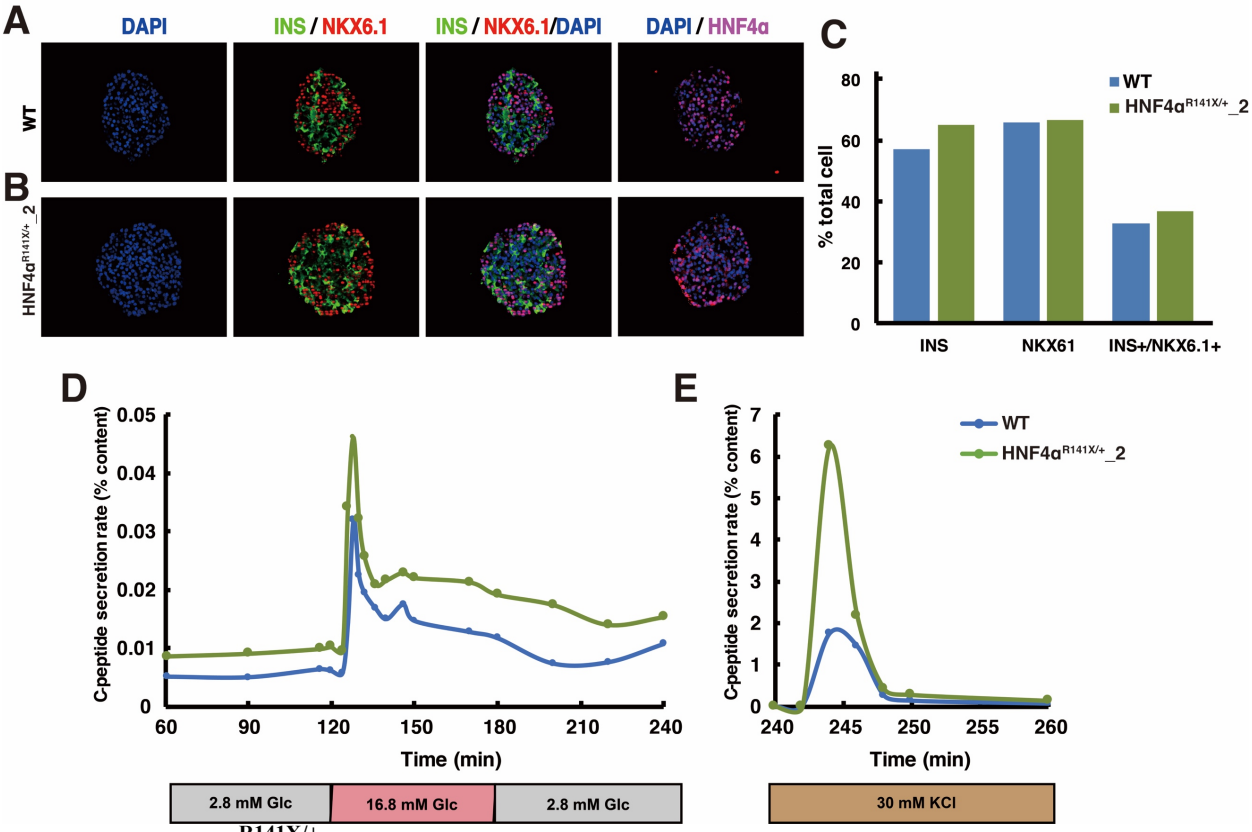


Figure 7. *HNF4α*$^{R141X/+}$ mutant cells secrete more insulin in response to high glucose levels at the functionally mature beta cell stage (FMB).

(A-B) IF staining of functionally mature beta cells (FMB) for (A) wild-type and (B) *HNF4α*$^{R141X/+}$ clone 2. Green stains for INS, red stains for NKX6.1, blue stains for DAPI, purple stains for HNF4α. (C) IF quantification of INS+, NKX6.1+, INS+/NKX6.1+ cells at FMB stage. (D-E) Perfusion results of FMB cell aggregates at (D) low and high glucose levels and (E) KCl stimulation.

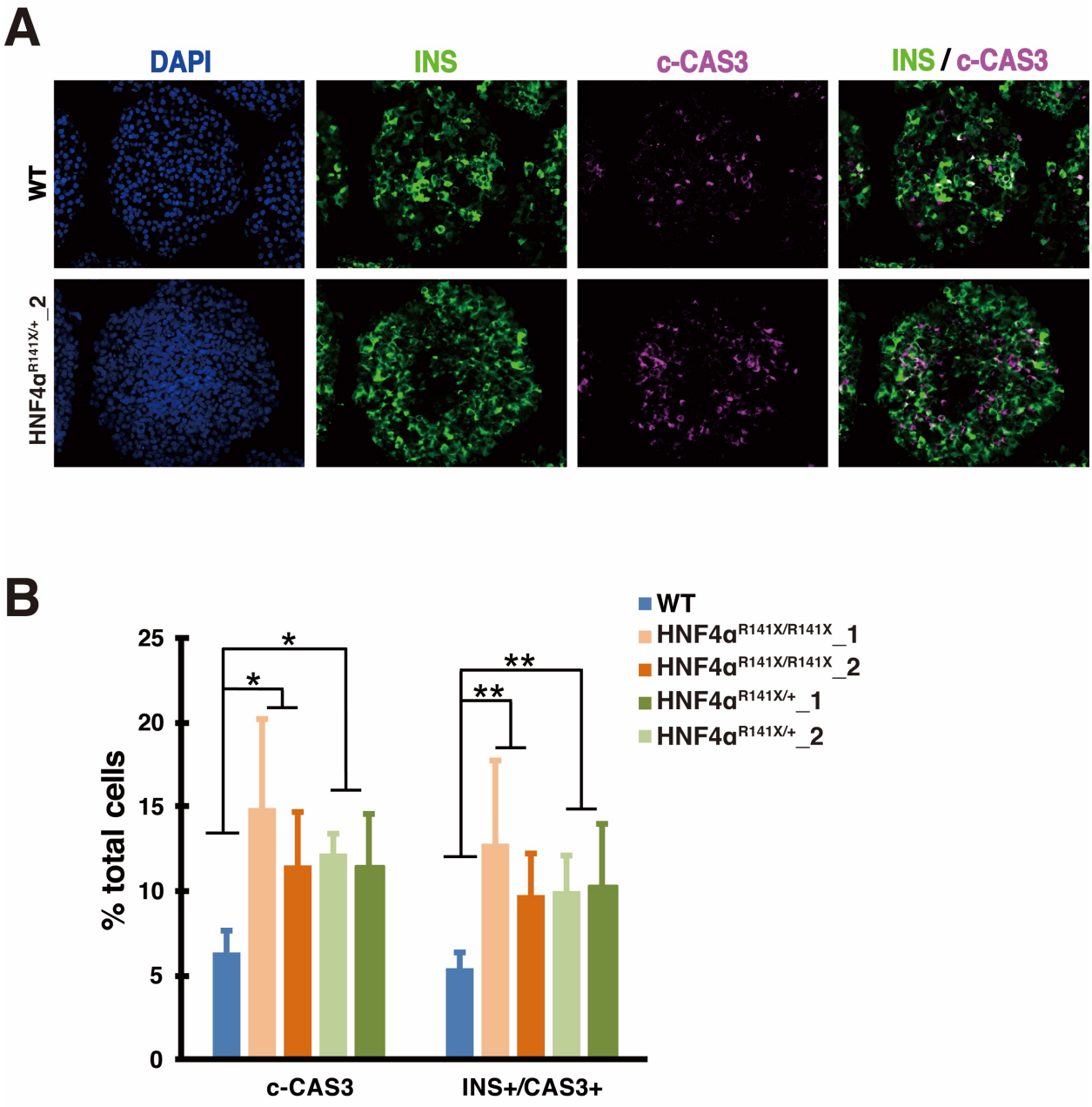


Figure 8. *HNF4α*^{R141X} mutants may more prone to cell death.
(A) IF staining of hESC-derived beta cell aggregates at IMB2 stage. Blue indicates DAPI, green indicates insulin (INS), pink indicates cleaved-caspase 3 (c-CAS3). (B) IF staining quantification of c-CAS3+ and c-CAS3+/INS+ cells. *p<0.05, **p<0.01.

DISCUSSION

Diabetes mellitus is an emerging global epidemic that affects over 387 million people worldwide [3]. It is a heterogeneous metabolic disease that has many subtypes, each with a different underlying molecular cause and clinical presentation. One such subtype, MODY1, is a form of monogenic diabetes caused by single base pair mutation in *HNF4α.* While it has been identified in patients and families, the underlying mechanism of MODY1 remains largely unknown. In addition, the phenotype observed in patients cannot be replicated in rodents by introducing *HNF4α* deletion [29,30,31,32]. The lack of understanding for MODY1 mechanism and the discrepancy between the human and rodent phenotype makes a MODY1 human *in vitro* model invaluable. Our studies show that through utilizing CRISPR/Cas9 technology in hESCs and a stepwise differentiation protocol to differentiate these cells into beta cells, our system provides a promising *in vitro* disease model to study MODY1.

Using a CRISPR/Cas9 dual-donor system, we were able to increase efficiency in obtaining $HNF4\alpha^{R141X/+}$ mutant clones. To validate our hESC-based MODY1 model, we investigated the ability of $HNF4\alpha^{R141X}$ mutants to express HNF4α and to undergo pancreatic induction and beta cell differentiation. We found that HNF4α expression decreases over time during beta cell differentiation course, with a more drastic decrease in $HNF4\alpha^{R141X/+}$ clones than the wild-type. This is explained by the auto-regulation loop of HNF4α, in which HNF4α binds to its own P2 promoter to enhance expression [50]. The morphology of $HNF4\alpha^{R141X}$ mutated cells resembled that of the wild-type cells with similar populations of PDX1+, NKX6.1+, and PDX1+/NKX6.1+ cells at the PE stage, suggesting that the mutation did not affect pancreatic induction. Furthermore, while $HNF4\alpha^{R141X}$ mutants had a lower percentage of NKX6.1+/INS+ cells comparing to the wild-

type cells at the IMB1 stage, this phenomenon was not observed in EP and IMB2 stages, suggesting that the difference was only transient. Our data suggests that beta cell differentiation was not greatly affected by *HNF4α*^{R141X} mutations.

Patients with MODY1 are characterized with neonatal HH, macrosomia, and early onset diabetes [18]. Similar to clinical presentation of MODY1 patients, the *HNF4α*^{R141X} mutants at the IMB2 stage, which likely corresponds to the neonatal stage *in vivo*, consistently exhibited elevated insulin secretion at low glucose and 30mM KCl-stimulation. At the age of 3 months to 8 years, patients are often treated with diazoxide for neonatal hyperinsulinemia [19]. At the IMB2 stage, *HNF4α*^{R141X} mutants also showed a drastic decrease in insulin secretion in response to diazoxide, as opposed to the negligible insulin secretion decrease as seen in wild-type cells. At the FMB stage *in vitro*, both wild-type cells and *HNF4α*$^{R141X/+}$ mutant cells displayed glucose responsiveness, an indicator of beta cell functional maturity. Importantly, *HNF4α*$^{R141X/+}$ mutant cells consistently hypersecrete insulin in a low glucose environment, upon glucose-stimulation, and with KCl stimulation. Altogether, these results show that *in vitro*-generated *HNF4α*$^{R141X/+}$ beta cells not only exhibit functional maturity, but also present phenotypes that closely resemble clinical phenotypes of MODY1 patients.

A number of recent studies have suggested ER stress as a possible cause of diabetes due to the huge burden on the ER to synthesize insulin [60]. When the level of secretion exceeds the ability of the cell to maintain ER homoeostasis, the unfolded protein response (UPR) is normally activated to restore ER homeostasis. However, when the UPR is insufficient to restore ER homeostasis, apoptosis is normally activated [61]. A recent study has also demonstrated that lack of HNF4α function in MODY1 patients results in Ca^{2+} signaling and insulin release disruption in beta cells by altering ER Ca^{2+} homeostasis [28]. We found that *HNF4α*$^{R141X/+}$ mutants had elevated

number of cells expressing c-CAS3. Increased beta cell death has been linked to ER stress, suggesting the possibility that increased ER stress eventually leads to elevated beta cell death and early onset diabetes observed in MODY1 patients. To confirm this connection between ER stress, altered Ca^{2+} signaling, and the MODY1 phenotype, in future studies we plan to examine whether elevated levels of apoptosis markers is observed in later stages of differentiation. We also plan to transplant our hESC-derived beta cells into the mouse kidney capsule to see whether the same effect is observed *in vivo*. While we were able to generate an *in vitro* model to study $HNF4\alpha^{R141X/+}$-mediated MODY1, many questions still remain unanswered. We hope that by using the MODY1 *in vitro* model we generated in this study, we will have the tool to investigate the underlying molecular cause of MODY1.

MATERIALS AND METHODS

hESC Cell Culture

The H1 hESC line was obtained from WiCell Research Institute, Inc. (Madison, WI). It was cultured on 1:100 diluted growth factor reduced Matrigel matrix. The cells were cultured in mTeSR with 1% penicillin-streptomycin (p/s) and the medium was changed daily. The culture was grown in an open system incubator at 37°C and 5% CO_2.

DNA Transfection with CRISPR/Cas9 and Clone Selection

Unless otherwise indicated, cell culture dissociation was achieved by the following: cells were washed with 1x DPBS and treated with Accutase for 3-5 minutes at 37°C and quenched with DMEM/F12 (with glutamine and HEPES). The cell suspension was centrifuged for 5 minutes at 400xg. The supernatant was removed and the cell pellet was suspended in mTeSR with Y-27632 (1:1000). Cell count was obtained by diluting 1:10 in DPBS and counted with Scepter cell counter.

1.5 x 10^6 cells per well of a 6-well plate was seeded 18~20 hours before transfection. Prior to transfection, pX458 Cas9/sgRNA plasmid containing the desired gRNA was prepared using Golden-Gate sgRNA cloning protocol. X-tremeGENE HP DNA Transfection Reagent was used to perform transfection. 2μg of R141X donor template, 6μg mR141X donor template, 2μg pX458 Cas9/sgRNA plasmid, 6μl XtremeGENE9 Transfection Reagent were combined with enough volume of OptiMEM to make the final mixture to 100μl before being incubated together at room temperature for 20 minutes (Table 1). The transfection mixture was added to culture with fresh mTeSR, Y-27632 (1:1000), and SRC7 (1:10000) and incubated overnight at 37°C.

The transfected culture was then dissociated with Accutase, suspended in 0.5% bovine serum albumin (BSA) in DPBS, run through a 35μm cell strainer, and sorted by fluorescence

activated cell sorting (FACS). 5000-7000 green fluorescence protein (GFP) positive cells were sorted into each well of a 6-well plate. Colonies were picked 4-7 days after sorting and sequencing was obtained through polymerase chain reaction (PCR) with appropriate primer pairs (Table 1).

in vitro Differentiation of hESCs

The H1 culture was dissociated with Accutase, seeded at 0.65 x 10^6 cells per well in 6-well Matrigel-coated plate, and maintained in mTeSR with penicillin streptomycin (p/s) (1:100). 72 hours after seeding, the H1 culture was dissociated with Accutase for 4 minutes and 5.5 x 10^6 cells were placed in 5.5 ml of mTeSR with Y-27632 (1:1000) in 6-well ultra-low attachment plates. The culture suspension was then placed on an orbital shaker at 100 rpm in a 37°C incubator for 24 hours. Cell aggregates were washed with Stage 1 basal media (see below), then submerging into 5.5 ml Stage 1 media with growth factors and placed on orbital shaker at 100 rpm. The culture in suspension was maintained with following basal media conditions: Stage 1-2 (D0-5): MCDB131 with 1x Glutamax, 15mM glucose, 1.5g/l $NaHCO_3$, and 0.5% BSA. Stage 3-4 (D6-10): MCDB131 with 1x Glutamax, 15mM glucose, 2.5g/l $NaHCO_3$, and 2% BSA. Stage 5-6 (D11-20): MCDB131 1x Glutamax, 20mM glucose, 1.5g/l $NaHCO_3$, and 2% BSA. Stage 7 (D21-39): MCDB131, 1x Glutamax, 5.5mM glucose, 1.5g/l $NaHCO_3$, and 2% BSA. In addition to the basal media, growth factors and conditions were added at each stage as follows: Stage 1 (D0-2): 100ng/ml activin A (AA) and 25ng/ml wnt3α for one day followed by 100ng/ml AA for 2 days. Stage 2 (D3-5): 50ng/ml FGF7 and 0.25mM ascorbic acid (VitC). Stage 3 (D6-7): insulin-transferrin-selenium ethanolamine (ITS-X) (1:200), 50ng/ml FGF7, 0.25mM VitC, 0.25μM SANT-1, 1μM retinoic acid (RA), 100nM LDN193189, and 200nM TPB. Stage 4 (D8-10): ITS-X (1:200), 2ng/ml FGF7, 0.25mM VitC, 0.25μM SANT-1, 0.1μM RA, 200nM LDN193189, 100nM TPB, and rotation

speed increased to 118rpm. Stage 5 (D11-14): ITS-X (1:200), 1μM T3, 10μM ALK5 inhibitor II (ALK5i), 0.25μM SANT-1, 0.05μM RA, 100nM LDC193189, 10μM $ZnSO_4$, and 10μg/ml heparin. Stage 6 (D14-20): ITS-X (1:200), 1μM T3, 10μM ALK5i, 100nM LDN193189, 100nM gamma secretase inhibitor XX (GSiXX), and 10 μg/ml heparin. Stage 7 (D21-24 without resize): ITS-X (1:200), 1μM T3, 10μM ALK5i, 10μM $ZnSO_4$, 1nM N-acetyl cysteine (N-Cys), 10μM Trolox, and 2μM R248.

To improve beta cell maturation, aggregates were resized at D21 by dissociating with Accutase, $3x10^6$ cells were placed in each well at 100rpm with S7 basal media, CloneR (1:100), 10μg/ml heparin, 10μM $ZnSO_4$, 1x MEM nonessential amino acids, Trace Elements A (1:1000), and Trace Elements B (1:1000). Media was changed daily with the described composition without CloneR after first day of resuspension. 24 hours after re-aggregation, the rotation speed was increased to 118rpm and cultured until D39 for endpoint analysis.

Cryosection of hESC-Derived Beta Cells

Cell aggregates were collected from suspension culture, washed with 1x DPBS twice, and then fixed with 4% paraformaldehyde (PFA) at room temperature for 20 minutes. The sample was washed with 1x DPBS twice then submerged in 30% sucrose at 4°C overnight for cryoprotection. The sample was embedded in optimal cutting temperature compound (O.C.T.) and kept in -80°C until sectioning. hESC-derived beta cell samples embedded in OCT were cryosectioned using Leica CM3050 S research cryostat with 10μm thickness and kept at -80°C until use.

Immunofluorescence Staining and Quantification

Immunofluorescence (IF) staining was achieved by washing the sample sections with 1xDPBS for 10 minutes twice, permeabilizing with 0.15% Triton-X 100 in PBS for 30 minutes, and blocking with blocking buffer (1% natural donkey serum (NDS) in 0.15% Triton-X 100) for 1 hour. The sections were then incubated with monoclonal primary antibodies (see Table 2) for 2 hours at room temperature or overnight at 4°C. The sections were then washed with blocking buffer for 10 minutes twice and incubated with secondary antibodies (1:200) and DAPI (1:1000) for 1 hour at room temperature (Table 2). After two washes of 1xDPBS for 10 minutes, the fluorescence was preserved with Vectashield mounting medium. Images of IF stained slides were taken with ZEISS Apotome and processed with Zeiss Zen 2. The images were quantified using HALO image analysis software.

Flow Cytometry

Differentiated cell aggregates were dissociated with Accutase for 5 minutes at 37°C, resuspended, and incubated for another 5 minutes. A short spin was performed to collect the supernatant while fresh Accutase was added to the remained aggregates for incubation. Incubation and suspension were repeated until all aggregates were dissociated into a single cell suspension. The cell suspension was then quenched with 1xDPBS and spun down. Unless otherwise specified, all centrifuging was done at 5000rpm for 5 minutes at 4°C. Cell pellets were resuspended in 250µl BD Cytofix/Cytoperm Solution and incubated on ice for 20 minutes. Samples were spun down and washed twice with BD Perm/Wash buffer then incubated in conjugated antibodies for 1 hour on ice (Table 3). After incubation, cells were spun down and washed twice with BD Perm/Wash buffer. Cell pellets were resuspended in 500µl of BD Perm/Wash buffer and processed through a cell strainer. The results were gated by the corresponding isotype (Table 3).

Western Blot

Differentiated cell aggregates were collected and washed with 1x DPBS twice. Cell aggregates were incubated on ice in RIPA buffer (10mM Tris, pH 8; 100mM NaCl, 1mM EDTA, 1mM EGTA, 10% NP-40, 0.1% SDS, 0.5% deoxycholate, 1x proteinase inhibitor, 1mM PMSF) for 30 minutes. The aggregates were sonicated with Diagenode Bioruptor for 10 cycles, 30 seconds on and 30 seconds off. Cell pellets were removed by centrifuging at max speed at 4°C for 10 minutes. Protein concentration was quantified using a Micro BCA Assay (Thermo Fisher). Equal amounts of protein were mixed with 3x Laemmli buffer and boiled for 5 minutes to ensure complete denaturation. The samples were electrophoresed on a 5% stacking gel and 12.5% separation gel, then transferred to PVDF membranes. Blocking was performed with PBST with 5% dry milk for 1 hour at room temperature. Membranes were then incubated with primary antibody overnight at 4°C, followed by 1 hour secondary antibody incubation at room temperature. Antibodies included HNF4α (Santa Cruz, sc-6556, 1:1000) and GAPDH (Ambion, AM4300, 1:4000). Western blot quantification is done using an Image Studio Lite. Band intensity was first normalized using GAPDH, then by band intensity of corresponding PE stage.

GSIS Perfusion

To access the GSIS response of hESC-derived beta cells, 75 aggregates were collected from suspension culture and used to perform perfusion using the Biorep Perfusion System. Day 24 samples were starved with Krebs-Ringer-Bicarbonate solution (KRB) with 2.8 mM glucose for 90 minutes, then treated with 100mM diazoxide for 20 minutes, followed by KRB with 30mM KCl (Table 4). Day 39 samples were starved at 2.8mM glucose in KRB for 2 hours, followed by

1 hour of 16.8mM glucose, 1 hour of 2.8mM glucose, then 30 minutes of 30mM KCl. The aggregates were sonicated in KRB with a Diagenode Bioruptor for 10 cycles, 30 seconds on and 30 seconds off.

C-peptide Quantification

C-peptide quantification of the perfusion samples were done using the STELLUX Chemi Human C-peptide ELISA kit. C-peptide reading was normalized using total C-peptide from cell aggregate lysates.

Data Analysis

All data presented in the figures were representative of at least 3 replicates, with the exception of FACS and perfusion data. All averages, standard deviations, and p-values of student's t-test were all calculated and graphed using Microsoft Excel. Statistical significance was indicated with *$p<0.05$, **<0.01, ***<0.001. All images were processed with Adobe Photoshop CC 2017 and assembled with Adobe Illustrator CC 2017.

Table 1. List of Plasmids and Primers

Name	Sequence
PCR forward primer	CCAGCTGAGTTAGAGGCCAT
PCR reverse primer	AAACTGGGCCATGTGAAACC
PAM mutation donor plasmid	GTGTGGGGGATCCCTGGGTGGGTGGCAGGATCAC CCCGGTACCTGTCGGGACAGCACCTCCGCCTGCA GGAGCGCATTGATGGAGGGCAGGCTGCTGTCC
PAM & R141X mutation donor plasmid	GTGTGGGGGATCCCTGGGTGGGTGGCAGGATCAC CCCGGTACCTGTCAGGACAGCACCTCCGCCTGCA GGAGCGCATTGATGGAGGGCAGGCTGCTGTCC
R141X gRNA forward primer	caccgACCCCGGTACCTGTCGGGAC
R141X gRNA reverse primer	aaacGTCCCGACAGGTACCGGGGTc

Table 2. List of Antibodies for Immunofluorescence Staining

Primary Antibodies				
Name	**Isotype**	**Company**	**Catalogue #**	**Dilution**
Cleaved Caspase-3 (Asp175) (5A1E)	Rabbit monoclonal IgG	Cell Signaling Technology, Inc	9664s	1:250
HNF-4α (C-19)	Goat polyclonal IgG	Santa Cruz	sc-6556	1:1000
Insulin	Guinea pig polyclonal IgG	DAKO	A0564	1:500
NKX6.1	Mouse monoclonal IgG	DSHB	F55A10	1:300
PDX1	Goat polyclonal IgG	Abcam	ab47383	1:500
Secondary Antibodies				
Name	**Isotype**	**Company**	**Catalogue #**	**Dilution**
Alexa Fluor® 488 AffiniPure Donkey Anti-Goat IgG (H+L)	Goat polyclonal IgG	Jackson Immuno Research	705-545-147	1:200
Alexa Fluor® 488 AffiniPure Donkey Anti-Guinea Pig IgG (H+L)	Guinea pig polyclonal IgG	Jackson Immuno Research	706-545-148	1:200
Alexa Fluor® 647 AffiniPure Donkey Anti-Mouse IgG	Mouse polyclonal IgG	Jackson Immuno Research	715-605-151	1:200
Cy™3 AffiniPure Donkey Anti-Goat IgG (H+L)	Goat polyclonal IgG	Jackson Immuno Research	705-165-147	1:200
Cy™3 AffiniPure Donkey Anti-Mouse IgG	Mouse polyclonal IgG	Jackson Immuno Research	715-165-151	1:200
Cy™3 AffiniPure Donkey Anti-Rabbit IgG (H+L)	Rabbit polyclonal IgG	Jackson Immuno Research	711-165-152	1:200
Hoechst 33342, trihydrochloride, trihydrate		MP (Molecular Probes)	H3570	1:1000

Table 3. List of Flow Cytometry Antibodies

Name	Isotype	Company	Catalogue #	Dilution
Insulin Alexa Fluor® 647 rabbit conjugate	Rabbit IgG	Cell Signaling	9008S	1:50
NKX6.1 PE mouse conjugate	Mouse IgG_1, κ	BD	563023	1:25
PDX-1 Alexa Fluor® 488 Mouse conjugate	Mouse IgG_1, κ	BD Pharmingen	562274	1:25
Alexa Fluor® 488 Mouse IgG1 κ Isotype Control	Mouse IgG_1, κ	BD Pharmingen	557782	1:25
Alexa Fluor® 647 rabbit IgG XP® Isotype Control	Rabbit IgG	Cell Signaling	2985S	1:50
PE Mouse IgG1, κ Isotype Control	Mouse IgG_1, κ	BD	556650	1:25

Table 4. Krebs-Ringer-Bicarbonate Solution for Perfusion Assay

Component	Low glucose	High glucose	High KCl
NaCl	130 mM	130 mM	130 mM
KCl	5 mM	5 mM	30 mM
$CaCL_2$	1.2 mM	1.2 mM	1.2 mM
$MgCl_2$	1.2 mM	1.2 mM	1.2 mM
KH_2PO_4	1.2 mM	1.2 mM	1.2 mM
Hepes: pH7.4	20 mM	20 mM	20 mM
$NaHCO_3$	25 mM	25 mM	25 mM
BSA	0.10%	0.10%	0.10%
Glucose	2.8 mM	16.8 mM	2.8 mM

REFERENCES

[1] American Diabetes Association. Diagnosis and Classification of Diabetes Mellitus. *Diabetes Care*. 2014; 37: S81-S90.

[2] Center for Disease Control and Prevention. National Diabetes Statistics Report, 2017. Atlanta, GA: Centers for Disease Control and Prevention, US Department of Health and Human Services. 2017.

[3] Centers for Disease Control and Prevention. About Underlying Cause of Death 1999–2015. CDC WONDER Database. 2017.

[4] Katsarou A, Gudbjörnsdottir S, Rawshani A, Dabelea D, Bonifacio E, Anderson BJ, Jacobsen LM, Schatz DA, Lernmark Å. Type 1 diabetes mellitus. *Nature Reviews Disease Primers*. 2017; 3: 17016.

[5] American Diabetes Association. Glycemic Targets. *Diabetes Care*. 2016; 39 (Supplement 1): S39-S46.

[6] DeFronzo RA. From the Triumvirate to the Ominous Octet: A New Paradigm for the Treatment of Type 2 Diabetes Mellitus. *Diabetes*. 2009; 58(4): 773-795.

[7] DeFronzo RA, Ferrannini E, Groop L, Henry RR, Herman WH, Holst JJ, Hu FR, Kahn CR, Raz I, Shulman GI, Simonson DC, Testa MA, Weiss R. Type 2 diabetes mellitus. *Nature Reviews Primers*. 2015; 1: 15019.

[8] Holman RR, Turner RC. Optimizing blood glucose control in type 2 diabetes: an approach based on fasting blood glucose measurements. *Diabetes Med.*1988; 5: 582-588.

[9] DeFronzo RA, Eldor R, Abdul-Ghani M. Pathophysiologic approach to therapy in patients with newly diagnosed type 2 diabetes. *Diabetes Care*. 2013; 36 (supplement 2): S127-S138.

[10] Ledermann HM. Is maturity onset diabetes at young age (MODY) more common in Europe than previously assumed? *Lancet*. 1995; 345 (8950): 648.

[11] Vazillaire M, Froguel P. Monogenic diabetes in the young, pharmacogenetics and relevance to multifactorial forms of type 2 diabetes. *Endocrine Reviews*. 2008; 29(3): 254-264.

[12] Online Mendelian Inheritance in Man, OMIM. Maturity-onset diabetes of the young; MODY. Johns Hopkins University, Baltimore, MD. 2016; 60639: 60639.

[13] Misra S, Hattersley AT. Chapter 18 monogenic causes of diabetes. In: Holt R, Cockram C, Flyvbjerg A, Godlstein B, editors. *Textbook of diabetes*. 2017; 5(5): 243

[14] Yang Y, Chan L. Monogenetic diabetes: what it teaches us on the common forms of type 1 and type 2 diabetes. *Endocrin Reviews*. 2016; 37(3): 190-222.

[15] Njolstad PR, Sovik O, Cuesta-Munoz A, Bjorkhaug L, Massa O, Barbetti F, Undlien DE, Shiota C, Magnuson MA, Molven A, Matschinsky FM, Bell GI. Neonatal diabetes mellitus due to complete glucokinase deficiency. *N. Engl. J. Med.* 2001; 344: 1588–1592.

[16] Stoffers DA, Zinkin NT, Stanojevic V, Clarke WL, Habener JF. Pancreatic agenesis attributable to a single nucleotide deletion in the human IPF1 gene coding sequence. *Nature Genetics*. 1997; 15(1): 104-110.

[17] Colclough K, Bellanne-Chantelot C, Saint-Martin C, Flanagan SE, Ellard S. Mutations in the genes encoding the transcription factors hepatocyte nuclear factor 1 alpha and 3 alpha in maturity-onset diabetes of the young and hyperinsulinemic hypoglycemia. *Human Mutation*. 2013; 34(5): 669-685.

[18] Pearson ER, Boj SF, Steele AM, Barrett T, Stals K, Shield JP, Ellard S, Ferrer J, Hattersley AT. Macrosomia and hyperinsulinaemic hypoglycaemia in patients with heterozygous mutations in the HNF4A gene. *Public Library of Science Medicine*. 2007; 4(4): 118.

[19] Flanagan SE, Kapoor RR, Mali G, Cody D, Murphy N, Schwahnn B, Siahanidou T, Banerjee I, Akcay T, Rubio-Cabezas O, Shield JPH, Hussain K, Ellard S. Diazoxide-responsive hyperinsulinemic hypoglycemia caused by HNF4A gene mutations. *European Journal of Endocrinology*. 2010; 162(5): 987-992.

[20] Pearson ER, Pruhova S, Tack CJ, Johansen A, Castleden HA, Lumb PJ, Wierzbicki AS, Clark PM, Lebl J, Pedersen O, Ellard S, Hansen T, Hattersley AT. Molecular genetics and phenotypic characteristics of MODY caused by hepatocyte nuclear factor 4alpha mutations in a large European collection. *Diabetologia*. 2005; 48(5): 878–885.

[21] Fajans SS, Brown MB. Administration of sulfonylureas can increase glucose-induced insulin secretion for decades in patients with maturity-onset diabetes of the young. *Diabetes Care*. 1993; 16: 1254–61.

[22] Sladek, FM, Zhong, WM, Lai, E, Darnell, JE Jr. Liver-enriched transcription factor HNF-4 is a novel member of the steroid hormone receptor superfamily. *Genes Development.* 1990: 4(12B): 2353–2365.

[23] Mangelsdorf, DJ, Evans RM. The RXR heterodimers and orphan receptors. *Cell*. 1995: 83, 841–850.

[24] Kuo CJ, Conley PB, Chen L, Sladek FM, Darnell JE, Crabtree GR. A transcriptional hierarchy involved in mammalian cell-type specification. *Nature*. 1992; 355: 457–461.

[25] Thomas H, Jaschkowitz K, Bulman M, Fraling TM, Mitchell SM, Roosen S, Lingott-Frieg A, Tack CJ, Ellard S, Ryffel GU, Hattersley AT. A distant upstream promoter of the HNF-4alpha gene connects the transcription factors involved in maturity-onset diabetes of the young. *Human Molecular Genetics*. 2001; 10(19): 2089-2097.

[26] Odom DT, Zizlsperger N, Gordon DB, Bell GW, Rinaldi NJ, Murray HL, Volkert TL, Schreiber J, Rolfe PA, Gifford DK, Fraenkel E, Bell GI, Young RA. Control of pancreas and liver gene expression by HNF transcription factors. *Science*. 2004; 303(5662): 1378–1381.

[27] Gupta RK, Gao N, Gorski RK, White P, Hardy OT, Rafiq K, Brestelli JE, Chen G, Stoeckert CJ Jr, Kaestner KH. Expansion of adult beta-cell mass in response to increased metabolic demand is dependent on HNF-4alpha. *Genes and Development*. 2007; 21(7): 756-769.

[28] Moore BD, Jin RU, Lo H, Jung M, Wang H, Battle MA, Wolheim CB, Urano F, Mills JC. Transcriptional regulation of x-box-binding protein one (XBP1) by hepatocyte nuclear factor 4α (HNF4A) is vital to beta-cell function. *Journal of the Biological Chemistry*. 2016; 291(12): 6146-6157.

[29] Byrne MM, Sturis J, Menzel S, Yamagata K, Fajans SS, Dronsfield MJ, Bain SC, Hattersley AT, Velho G, Froguel P, Bell GI, Polonsky KS. Altered insulin secretory responses to glucose in diabetic and nondiabetic subjects with mutations in the diabetes susceptibility gene MODY3 on chromosome 12. *Diabetes.* 1996; 45(11): 1503–1510.

[30] Yamagata K, Furuta H, Oda N, Kaisaki PJ, Menzel S, Cox NJ, Fajans SS, Signorini S, Stoffel M, Bell GI. Mutations in the hepatocyte nuclear factor-4a gene in maturity-onset diabetes of the young (MODY1). *Nature*. 1996;384(6608): 458-460.

[31] Hayhurst GP, Lee Y-H, Lambert G, Ward JM, Gonzalez FJ. Hepatocyte nuclear factor 4a (Nuclear Receptor 2A1) is essential for maintenance of hepatic gene expression and lipid homeostasis. *Molecular and Cellular Biology*. 2001; 21(4): 1393–1403.

[32] Miura A, Yamagata K, Kakei M, Hatakeyama H, Takahashi N, Fukui K, Nammo T, Yoneda K, Inoue Y, Sladek FM, Magnuson MA, Kasai H, Miyagawa J, Gonzalez FJ, Shimomura I. Hepatocyte nuclear factor-4alpha is essential for glucose-stimulated insulin secretion by pancreatic beta-cells. *Journal of the Biological Chemistry*. 2006; 281(8): 5246-5247.

[33] D'Amour KA, Bang AG, Eliazer S, Kelly OG, Agulnick AD, Smart NG, Moorman MA, Kroon E, Carpenter MK, Baetge EE. Production of pancreatic hormone-expressing endocrine cells from human embryonic stem cells. *Nature Biotechnology*. 2006; 24(11), 1392–1401.

[34] Schulz TC, Young HY, Agulnick AD, Babin MJ, Baetge, Bang AG, Bhoumik A, Cepa I, Cesario RM, Haakmeester C, Kadoya K, Kelly JR, Kerr J, Martinson LA, McLean AB, Moorman MA, Payne JK, Richardson M, Ross KG, Sherrer ES, Song X, Wilson AZ, Brandon EP, Green CE, Kroon EJ, Kelly OG, D'Amour KA, Robins AJ. A scalable system for production of functional pancreatic progenitor from human embryonic stem cells. *Public Library of Science one*. 2012; 7(5): e37004.

[35] Reania A, Bruin JE, Riedel MJ, Mojibian M, Asadi A, Xu J, Gauvin R, Narayan K, Karanu F, O'Neil JJ, Ao Z, Warnock GL, Kieffer TJ. Maturation of human embryonic stem cell-derived pancreatic progenitors into functional islets capable of treating pre-existing diabetes in mice. *Diabetes*. 2012; 61(8): 2016-2029.

[36] Pagliuca FW, Milman JR, Gurtler M, Segel M, Van Dervort A, Ryu JH, Peterson QP, Greiner D, Melton DA. Generation of functional human pancreatic β cells in vitro. *Cell*. 2015; 159(2): 428-439.

[37] Reania A, Bruin JE, Arora P, Rubin A, Batushansky I, Asadi A, O'Dwyer S, Quiskamp N, Mojibian M, Albrecht T, Yang YHC, Johnson JD, Kieffer TJ. Reversal of diabetes with insulin-producing cells derived in vitro from human pluripotent stem cells. *Nature Biotechnology*. 2014; 32: 112101133.

[38] Benninger RKP, Head WS, Zhang M, Satin LS, Piston DW. Gap junctions and other mechanisms of cell-cell communication regulate basal insulin secretion in the pancreatic islet. *Journal of Physiology*. 2011; 589: 5453–5466.

[39] Stendahl JC, Kaufman DB, Stupp SI. Extracellular matrix in pancreatic islets: relecance to scaffold design and transplantation. *Cell Transplantation*. 2009; 18(1): 1-12.

[40] Velazco-Cruz L, Song J, Maxwell KG, Goedegebuure MM, Augsornworawat P, Hogrebe NJ, Milman JR. Acquisition of dynamic function in human stem cell-derived β cells. *Stem Cell Reports*. 2019; 12(2): 351-365.

[41] Pagliuca FW, Millman JR, Gurtler M, Segel M, Van Dervort A, Ryu JH, Peterson QP, Greiner D, Melton DA. Generation of functional human pancreatic b cells in vitro. *Cell*. 2014; 159, 428–439.

[42] Jiang GQ, Lee U, Sladek FM. Proposed mechanism for stabilization of nuclear receptor DNA binding via protein dimerization. *Molecular and Cellular Biology*. 1997; 17(11): 6535-6554.

[43] Eeckhoute J, Formstecher P, Laine B. Maturity-onset diabetes of the young type 1 (MODY1)-associated mutations R154X and E276Q in hepatocyte nuclear factor 4alpha (HNF4alpha) gene impair recruitment of p300, a key transcriptional co-activator. *Molecular Endocrinology.* 2001; 15(7): 1200-1210.

[44] Laine B, Eeckhoute J, Suaud L, Briche I, Furuta H, Bell GI, Formstecher P. Functional properties of the R154X HNF-4α protein generated by a mutation associated with maturity-onset diabetes of the young, type 1. *FEBS Letters*. 2000; 479(2): 41-45.

[45] Nammo T, Yamagata K, Hamaoka R, Zhu Q, Akiyama T, Gonzalez F, Miyagawa J, Matsuzawa Y. Expression profile of MODY3/HNF-1a protein in the developing mouse pancreas. Diabetologia 2002; 45: 1142–1153.

[46] Shih DQ, Stoffel M. Dissecting the transcriptional network of pancreatic islets during development and differentiation. Proc Natl Acad Sci U S A 2001; 98: 14189–14191

[47] Gupta r, Vatamaniuk MZ, Lee C, Flaschen R, Fulmer J, Matchinsky FM, Duncan S, Kaestner K. The MODY1 gene HNF-4alpha regulates selected genes involved in insulin secretion. *J Clin Invest*. 2005; 115: 1006-1015.

[48] Rhee J, Inoue Y, Yoon Y, Puigserver P, Fan M, Gonzales FJ, Spiegelman B. Regulation of hepatic fasting reponse by PPARgamma coactivator-1alpha (PGC-1): requirement for hepatocyte nuclear factor-4alpha in gluconeogenesis. *Proc Natl Acd Sci USA*. 2003; 100: 4012-4017.

[49] Chen W, Chiang JY. Regulation of human sterol 27-hydroxylase gene (CYP27A1) by bile acids and hepatocyte nuclear factor-4alpha (HNF4alpha). *Gene*. 2003; 3131: 71-82.

[50] Sandovici I, Smith NH, Nitert DM, Ackers-Johnson M, Uribe-Lewis S, Ito Y, Jones RH, Marquez VE, Cairns W, Tadayvon M, O'Neill LP, Murrell A, Ling C, Constancia M, Ozanne SE. Maternal diet and aging alter the epigenetic control of a promoter – enhancer interaction at the Hnf4a gene in rat pancreatic islets. *Proc. Natl. Acad. Sci. USA*. 2011; 108(13): 5449-5454.

[51] Matsuoka TA, Artner I, Henderson E, Means A, Sander M, Stein R. The MafA transcription factor appears to be responsible for tissue-specific expression of insulin. *Proc. Natl. Acad. Sci. USA*. 2004; 101: 2930-2933.

[52] Hang Y, Yamamoto T, Benninger RK, Brissova M, Guo M, Bush W, Piston DW, Powers AC, Magnuson M, Thurmond DC, Stein R. The MafA transcription factor becomes essential to islet beta-cells soon after birth. *Diabetes*. 2014; 63: 1994-2005.

[53] Zhang X, Moriguchi, Kajihara M, Esaki R, Harada A, Shimohata H, Oishi H, Hamada M, Morito N, Masegawa K, Kudo T, Engel JD, Yamamoto M, Takahashi S. MafA is a key regulator of glucose-stimulated insulin secretion. *Mol. Cell Biol.* 2005; 25: 4969-4976.

[54] Straub SG, Sharp GW. Glucose-stimulated signaling pathways in biphasic insulin secretion. *Diabetes Metab. Res. Rev.* 2002; 18(6): 451-463.

[55] Curry DL, Bennett LL, Grodsky GM. Dynamics of insulin secretion by the perfused rat pancreas. *Endocrinology*. 1968; 83(3): 1033-1048.

[56] Aridor M, Balch WE. Integration of endoplasmic reticulum signaling in health and disease. *Nature Medicine*. 1999; 5: 745-751.

[57] Eizirik DL, Cardozo AK, Cnop Miriam. The role for endoplasmic reticulum stress in diabetes mellitus. *Endocrine Reviews*. 2008; 29(1): 42-61.

[58] Araki E, Oyadomari S, Mori M. Impact of endoplasmic reticulum stress pathway on pancreatic beta-cells and diabetes mellitus. *Exp. Biol. Med (Maywood)*. 2003; 228(10): 1213-1217.

[59] Back SH, Kang SW, Hang J, Chung HT. Endoplasmic reticulum stress in the β-cell pathogenesis of type 2 diabetes. *Experimental Diabetes Research*. 2012; 2012: 11.

[60] Schuit FC, In't Veld PA, Pipeleers DG. Glucose stimulates proinsulin biosynthesis by a dose-dependent recruitment of pancreatic beta cells. *Proc Natl. Acad. Sci USA*. 1988; 85: 3865-3869.

[61] Kim I, Xu W, Reed JC. Cell death and endoplasmic reticulum stress: disease relevance and therapeutic opportunities. *Nat. Rev. Drug Discov.* 2008; 7: 1013-1030.